An Associative Polyelectrolyte End-Capped with Short Polystyrene Chains. Synthesis and Rheological Behavior

ARTICLE *in* MACROMOLECULES · APRIL 2000

Impact Factor: 5.8 · DOI: 10.1021/ma991410e

3 AUTHORS, INCLUDING:

Constantinos Tsitsilianis
University of Patras
129 PUBLICATIONS **2,558** CITATIONS

SEE PROFILE

An Associative Polyelectrolyte End-Capped with Short Polystyrene Chains. Synthesis and Rheological Behavior

Constantinos Tsitsilianis*

Department of Chemical Engineering, University of Patras, and Institute of Chemical Engineering and High-Temperature Chemical Processes, ICE-FORTH, P.O.Box 1414, 26500, Patras, Greece

Ilias Iliopoulos and Guylaine Ducouret

Laboratoire de Physico-chimie Macromoleculaire, UMR-7615, ESPCI, CNRS, Universite Pierre et Marie Curie, 10 rue Vauquelin, 75231 Paris Cedex 05, France

Received August 18, 1999; Revised Manuscript Received January 27, 2000

ABSTRACT: Polystyrene (PS) end-capped polyelectrolytes were prepared by modification of polystyrene−poly(*tert*-butyl acrylate)−polystyrene triblock copolymers synthesized via anionic polymerization. These amphiphilic polymers are associated in dilute aqueous solutions forming loose multimicellar clusters. At higher polymer concentrations an extensive intermicellar bridging occurs, leading to the formation of a transient network as revealed by the viscoelastic response of the system. The so-formed gel is characterized by low gel concentration, i.e., 0.2 wt %, yield stress, complex steady-shear viscosity profile, high plateau modules, and long relaxation times. These characteristics can be attributed to the highly hydrophobic character of the PS junctions and the stretched conformation of the polyelectrolyte bridges.

Introduction

Hydrophobically modified, or associative, water-soluble polymers are increasingly used as thickeners in aqueous formulations (paints, cosmetics, drilling fluids, etc.). They are based on a water-soluble backbone and bear a low fraction of highly hydrophobic side or end groups.[1−3] In most of the known examples the hydrophobic groups are either alkyl chains, from octyl to octadecyl, or contain an aromatic ring (phenyl, naphthyl, pyrenyl, etc.). Perfluorinated alkyl groups have also been used as hydrophobic moieties because of their higher hydrophobicity compared to that of the hydrogenated analogues.[4−6] In aqueous solution the hydrophobic groups self-associate and form micellar type aggregates. In the semidilute regime, these aggregates act as cross-linkers between the polymer chains, and an enhancement in the rheological properties is observed. Because of this, these copolymers are often referred to as *associative polymers*.[2]

Numerous types of associative graft copolymers, with the hydrophobes as side groups, have been proposed on the basis of either a nonionic water-soluble backbone[4,7−15] or a polyelectrolyte.[5,16−22] In this case, the hydrophobic units are introduced either by copolymerization of the hydrophilic and hydrophobic monomers or by chemical modification of a precursor water-soluble polymer. The latter method has been used to obtain hydrophobic derivatives of poly(sodium acrylate), HMPA.[5,16]

On the other hand, numerous studies have been devoted to end-capped nonionic polymers, i.e., linear polymers with hydrophobic groups at the two ends. By far, the most studied are the derivatives of poly(ethylene oxide), PEO.[2,6,23−27] Their associating behavior in aqueous solutions is now well understood. In dilute solution and above a critical aggregation concentration they form micellar type aggregates (flowers) into which both the alkyl ends of the polymer are involved.[23] At higher concentrations, larger multiflower aggregates are formed with some of the polymer chains forming bridges between the flowers. The basic aggregate, i.e., the flower, is in many aspects similar to the surfactant micelles. It forms a liquidlike core surrounded by the hydrophilic corona of the PEO chains. The alkyl ends are labile and can enter into and exit the hydrophobic core, but the characteristic time of this process is slower than for equivalent surfactants, of the order of 0.1 ms.[28] The aggregation number, i.e., the number of alkyl ends per flower, was estimated to be about 20, clearly smaller than for surfactant micelles.[2,24,29]

At higher polymer concentrations, when a transient network is formed, the end-capped associative polymers present a rather simple rheological behavior described by a single relaxation time.[2,6,23,25,30,31] The relaxation process can be related to the exit of one hydrophobic end of a bridging chain from the micellar type aggregate. On the contrary, associative graft copolymers present a more complex rheological behavior in aqueous solution with a broad relaxation spectrum.[32] In the latter, each polymer chain is expected to contribute with several side groups to a given hydrophobic aggregate. Another important difference between the end-capped and graft associative polymers is the characteristic exchange time for the enter/exit process of the alkyl groups to the hydrophobic flowerlike aggregate. This time is considerably slowed in the case of graft copolymers. For instance, it is higher than 10 ms for a HMPA with dodecyl side groups.[33,34]

To the best of our knowledge, very little is known about the behavior of end-capped associative polyelectrolytes.[35,36] Murphy et al.[36] have synthesized quaternized derivatives of poly(vinyl-2-pyridine) asymmetrically end-capped with alkyl chains, C*n*, with *n* varying from 4 to 16. They mainly focused on the adsorption properties of these polymers onto vesicles and on the resulting stabilization effects. On the other hand, Valint and Bock[35] reported the synthesis of a triblock copolymer with a poly(styrenesulfonate) as water-soluble central block and short poly(*tert*-butylstyrene) blocks to the ends. Nevertheless, they did not report on the associative rheological behavior of this triblock copolymer in water.

10.1021/ma991410e CCC: $19.00
Published on Web 03/24/2000

Scheme 1

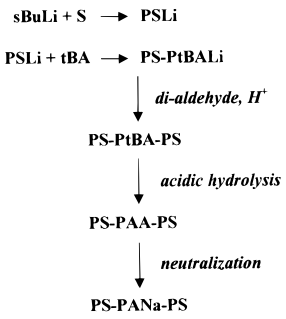

In the present work, we describe the synthesis, the characterization, and the first rheological results on the aqueous solution behavior of poly(sodium acrylate), PANa, derivatives end-capped with short polystyrene, PS, chains (Scheme 1). Because of the high glass transition, T_g, of polystyrene,[37] the PS end caps might form glasslike aggregates in the temperature range commonly explored for aqueous solutions ($10 \leq T \leq 70$ °C)—a situation similar to the "frozen micelles" formed by ionic block copolymers with PS as a short block.[38] That is expected to have some fundamental consequences on the behavior of these associative polymers in aqueous solution.

The paper is developed as follows. First we discuss the synthesis and the characterization of well-defined end-capped polyelectrolytes. Accordingly, we give information concerning the association phenomena of the polymer in aqueous solutions by using fluorescent measurements. After the steady-state flow behavior is presented, finally preliminary results of the viscoelastic behavior of the associative polymer solution are given. The possible association mechanism is discussed in the last section.

Experimental Section

Materials. Tetrahydrofuran (THF) free from protonic impurities was obtained according to standard procedures. Styrene was distilled twice from sodium wire under vacuum. *tert*-Butyl acrylate (tBA) was first vacuum distilled from calcium hydride and accordingly was treated with triethylaluminum (10% solution in heptane). Once a faint yellow was obtained, tBA was immediately vacuum distilled into burets. *sec*-Butyllithium was prepared from 2-chlorobutane and Li metal pieces in benzene. The dialdehyde terephthaldicarboxaldehyde (Aldrich) was recrystallized from water and used after prolonged drying.

Synthesis. The polystyrene−poly(*tert*-butyl acrylate)−polystyrene (PS−PtBA−PS) triblock copolymers were synthesized by anionic polymerization in a glass reactor under inert atmosphere. Polystyrene was polymerized first in THF in the presence of LiCl (5-fold) at −40 °C using *sec*-BuLi as initiator. The reaction medium was then cooled to −78 °C, and tBA monomer was added dropwise. A sudden color change confirmed that the initiation of the second monomer was fast and quantitative. After the completion of the polymerization of tBA and sampling out, a stoichiometric amount of dialdehyde was added slowly to the reaction medium containing the living PS−PtBA copolymer. The coupling reaction was allowed to be completed for 1 h. The alkoxide site was protonated by acetic acid.

Fractionation. Since the PS−PtBA−PS contains PS−PtBA diblock residuals, the final product was purified by fractional precipitation using THF as solvent and methanol−water (80:20 w/w) mixture as nonsolvent. The purified PS−PtBA−PS was redissolved in benzene and freeze-dried.

Hydrolysis of PS−PtBA−PS. The 23−1134−23 triblock copolymer was subjected to acidic hydrolysis in 1,4-dioxane with concentrated HCl at 80 °C for 18 h. The degree of hydrolysis of the resulted polymer was measured by ^{1}H NMR in a mixture of deuterated MeOH:$CHCl_3$ (3:1) and was found to be 98%. It should be mentioned here that the protons of the styrene and the remaining tBA units are not visible when the polymer is dissolved in polar solvents such as DMSO. The degree of hydrolysis was determined also by potentiometric titration by using 0.1 N NaOH. Since the hydrolyzed polymer is not soluble in water, a mixture of MeOH:H_2O (1:2) was used as solvent at 0.1 wt % concentration. The acid content was determined to be 80%. The same was found in a mixture DMF:H_2O (1:2).

Size Exclusion Chromatography. SEC was carried out using an apparatus equipped with two detectors: a differential refractometer (model 401, Water Associates) and a UV detector (Fasma 500, Rigas Labs). A set of three μ-styragel columns (10^3, 10^4, and 10^5 Å) was used, and the calibration curve was obtained by PS standards. The mobile phase was tetrahydrofuran, and the flow rate was 1 cm^3 min^{-1}. A deconvolution program was used to estimate the PS−PtBA residual.

Static Light Scattering. All the light scattering experiments were carried out using a thermally regulated (±0.1 °C) spectrogoniometer model SEM RD (Sematech, France) equipped with a He−Ne laser (633 nm). The refractive index increments dn/dc required the light scattering measurements were obtained by means of a Chromatic KMX-16 differential refractometer operating at 633 nm.

Fluorescence. Fluorescence measurements were conducted with a Perkin-Elmer luminescence spectrometer, LS 50 B, at 25 °C. Pyrene was employed as a micropolarity-sensitive probe. The excitation wavelength was 334 nm, and the emission spectrum was recorded between 350 and 500 nm. The intensities at 373 nm (I_1) and 384 nm (I_3) were used for measuring the I_1/I_3 ratio.

Rheology. Rheological measurements were performed on three different rheometers. Dynamic mechanical tests were ran on a strain controlled rheometer, Rheometric RFS-II, equipped with a cone/plate geometry (diameter = 50 mm, angle = 2°, truncation = 45 μm).

The flow properties of the solutions were studied with a stress controlled rheometer, Haake Rheostress RS-150, with cone/plate geometry (diameter = 35 mm, angle = 2°, truncation = 103 μm). For the less concentrated samples, $C_P \leq 0.1\%$, a Contraves Low-Shear-30 apparatus was used, equipped with a couette geometry (radius of cup = 6 mm, radius of conical cylinder = 5.5 mm). For all the experiments the temperature was fixed at 25 °C.

Sample Preparation. For the rheology measurements the solutions were directly prepared to the final desired concentration. The proper amount of polymer (acid form) was weighted in a screw-capped vial. First an equivalent amount of 0.1 N NaOH was added to neutralize the PAA units, and then water (Millipore) was added to the final volume. The samples were stirred for 24 h at room temperature and then heated for 24 h at 95−100 °C. They were shaken several times for short periods during the heating procedure. Finally they were allowed to cool to room temperature and the vials weighted. The concentration was corrected to take into account the loss of water (less than 1%) during the heating procedure. Good reproducibility in the rheological properties was found after that treatment. Hereafter the polymer concentration, C_P, is given in weight percent of the acid form.

For the fluorescence experiments the same procedure was followed for the preparation of the most concentrated samples (C_P = 0.1 and 0.2%). Samples of lower C_P were obtained by appropriate dilution of the 0.1% solution and equilibration at room temperature for several hours. An aliquot of an ethanolic stock solution of pyrene, 1.0×10^{-3} M, was added to the solutions to obtain a final pyrene concentration of 1.0×10^{-6} M.

The pH of the final solutions was dependent on the polymer concentration. For C_P = 0.1%, the pH was about 8 and decreased to ≈6 for the lowest concentrations used in fluorescence experiments.

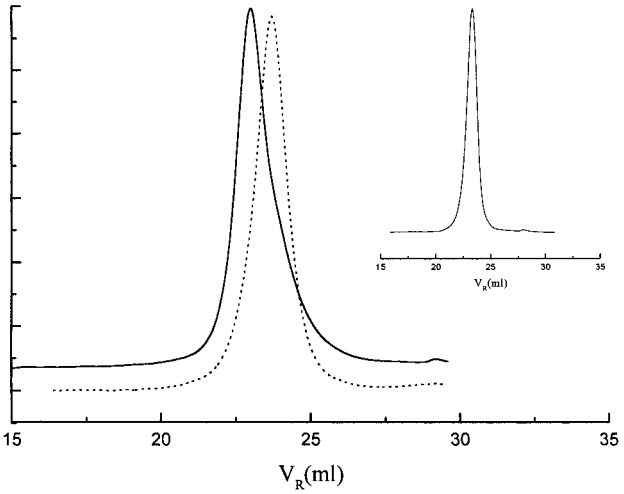

Figure 1. SEC chromatograms of PS−PtBA diblock precursor (dashed line) and PS−PtBA−PS triblock after coupling (full line). In the inset the SEC of the fractionated PS−PtBA−PS is presented.

Results and Discussion

Synthesis and Characterization. To produce well-defined PS end-capped polyeletrolytes, anionic polymerization techniques were employed by copolymerizing styrene and tBA. It is known that the second monomer can be modified in ionic groups after hydrolysis and neutralization. Although the synthesis of the diblock copolymers can be carried out by sequential addition of the monomers (starting from styrene),[39] the synthesis of a triblock copolymer with the PtBA block in the middle cannot be performed straightforward. The synthetic route we have followed is the synthesis of a diblock PS−PtBA precursor followed by a coupling reaction according to Scheme 1. Polystyrene short chains were synthesized first by using *sec*-BuLi as initiator at −40 °C in THF. The "living" polystyryl anions were used in a subsequent step to initiate the polymerization of tBA. The reaction medium was then cooled to −70 °C, and the tBA was added dropwise. To ensure "living" conditions during the polymerization of tBA, a 5-fold LiCl to the initiator was present in the medium.[40]

After total consumption of the monomer a small amount was sampled out and deactivated for the purpose of characterization. To the rest of the medium a coupling agent (dialdehyde) was introduced dropwise in stoichiometric amount. The latter was chosen since it is known that "living" butyl acrylic anions react effectively with dialdehydes, yielding multiblock copolymers with poly(*tert*-butyl acrylic) and polyvinylic sequences.[41] The coupling reaction leads to the synthesis of a PS−PtBA−PS triblock copolymer with identical PS block ends.

In Figure 1 an example of the chromatograms of the final product and the PS−PtBA precursor it originates from are illustrated. As can be seen, the triblock copolymer contains a small amount of uncoupled diblock precursor that is estimated to be 16−20% in all cases (Table 1). This residual was removed easily by fractionation, and the purified material (inset of Figure 1) was dissolved in benzene and freeze-dried.

Light scattering and ^{1}H NMR were used for the characterization of the samples. The M_w of the triblock copolymer is slightly higher than double the M_w of the diblock copolymer precursor due to the fractionation procedure. The final products are well-defined nearly monodisperse PS−PtBA−PS triblock copolymers with very low compositional heterogeneity, as was checked out by using simultaneously UV and IR detectors in the GPC analysis.

Accordingly, one of the polymers (sample 23-1134-23) was subjected to acid-catalyzed hydrolysis in order to modify the ester groups of the PtBA middle block to its acid from. The degree of hydrolysis of the resulting polymer was determined by potentiometric titration and was found to be 80%, remarkably lower than that obtained by ^{1}H NMR (98%). This discrepancy has also been observed for similar systems such as poly(acrylic acid)−poly(methyl methacrylate) block copolymers, and it is difficult to explain.[42] The triblock copolymer in its acid form was then neutralized with the equivalent amount of NaOH as determined from the potentiometric titration curve in order to maximize the solubility of the polymer. It is noted here that even a lower degree of neutralization (down to 60%) had no effect on the rheological behavior of the system. As has been observed for PS−PANa block copolymers, these materials cannot be dissolved directly in water.[43] This also observed for the PS−PANa−PS triblock copolymer of the present work. Therefore, the aqueous solutions were heated at 95−100 °C for ∼24 h and allowed progressively to cool at room temperature. Since the copolymer is constituted of PS hydrophobic and PANa hydrophilic segments, aggregation phenomena are expected to take place.

Fluorescence Measurements. Information about micellization phenomena of the PS−PANa−PS triblock copolymer in dilute aqueous solutions was obtained from steady-state fluorescence probe studies. A well-known method is to use pyrene as a fluorescent probe since its solubility in water is very low, and it is preferably solubilized into hydrophobic microdomains like the micellar cores are.[44−46] The I_1/I_3 intensity ratios of the first and third vibronic peaks in the fluorescence emission spectrum of pyrene were measured as a function of polymer concentration. The I_1/I_3 ratio is an index of the polarity of the pyrene microenvironment. In the presence of hydrophobic microdomains I_1/I_3 decreases from ∼1.8 (aqueous environment) to ∼1.2 when the pyrene probe is located mainly in the micellar aggregates.[45] This behavior also appeared in our system as illustrated in Figure 2. A gradual decrease of I_1/I_3 over a range of polymer concentrations of more than 1 decade is obtained. The end plateau of the I_1/I_3 curve cannot be reached because of the very high viscosity of the solutions. The midpoint of the transition occurs at $C_P = 2.5 \times 10^{-6}$ M, i.e., to a PS ends concentration $C_{PS} = 5 \times 10^{-6}$ M. In this type of system the I_1/I_3 data cannot be used for the determination of the critical aggregation concentration (cac). Because of the very low concentration in hydrophobic aggregates, of the same order as or lower than the pyrene concentration (10^{-6} M), the I_1/I_3 values might be strongly influenced by the partition of pyrene between PS aggregates and the aqueous phase.[43,44,47] However, the I_1/I_3 ratio can be used to ascertain the location of pyrene, and from the data of Figure 2, we can conclude that micellar type aggregates already exist at $C_P \approx 10^{-5}$ M (i.e., $C_P \cong 0.1\%$). Indeed, for diblock PS−PANa copolymers (half the length of our triblock) Astafieva et al.[43,48] found a cac $\sim 5 \times 10^{-7}$ M. Converting to triblock concentration, it results in cac $\sim 2.5 \times 10^{-7}$ M or cac ∼ 0.002% (accounted with M_n = 87 000). At higher polymer

Table 1. Molecular Characteristics of PS−PtBA−PS Triblock Copolymers

sample[a] PS−PtBA−PS	M_w(PS−PtBA)	M_w/M_n	coupling yield (%)[b]	M_w[c]	W_{PS} (%)[d]	M_w/M_n[c]	M_w(PS)[e]
10-632-10	36 000	1.15	83.9	83 000	2.45	1.13	1.016
23-1134-23	71 000	1.16	80.3	150 000	3.2	1.16	2.400

[a] The numerical indexes stand for the polymerization degree of each block. [b] By deconvolution of the GPC chromatograms. [c] Free from diblock residuals. [d] By ^{1}H NMR. [e] Calculated: $M_w(PS) = {}^1/_2(M_w W_{PS})$.

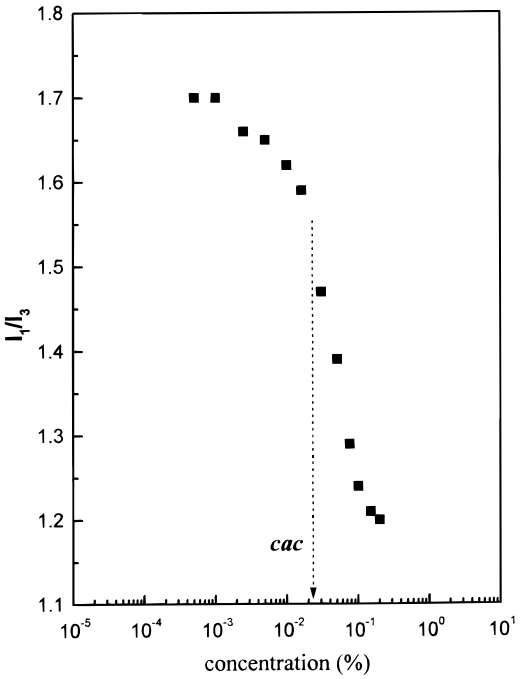

Figure 2. Variation of the intensity ratio I_1/I_3, in the fluorescence emission spectrum of pyrene, as a function of the PS−PANa−PS concentration in aqueous solution at 25 °C.

concentrations bridging between micelles is expected to lead to the formation of a network accompanied by interesting rheological behavior as will be demonstrated below.

Steady-State Shear Flow. Steady-state viscosity measurements were carried out in order to characterize the flow behavior of aqueous solutions of the neutralized end-capped polyelectrolyte. In Figure 3a the steady-state viscosity, η, versus shear rate, $\dot{\gamma}$, for a 1.0% solution is illustrated. A shear thinning effect can be observed in the entire shear rate region. That is due to the existence of a yield stress (see also Figure 3b,c). The measurable viscosity of a 1% solution at the lowest shear rate is about 5 orders of magnitude higher than that of water, revealing that this polymer exhibits strongly thickening efficiency.

The steady shear viscosity profile of the present PS-end-capped associative thickener differs remarkably from those of other associative end-capped polymers bearing a nonionic water-soluble middle block. As has been reported for PEO end-capped with either hydrogenated or fluorinated hydrophobes, a Newtonian plateau is observed, sometimes followed by a slightly shear-thickening behavior, prior to a dramatic drop of the viscosity at higher shear rates.[6,27] This behavior is not observed in our case. On the other hand, the viscosity curve exhibits a discontinuity at $\dot{\gamma} \approx 5\ s^{-1}$ which will be discussed in more detail in a following section.

The yield stress, τ_y, can be seen more clearly when the shear stress is plotted as a function of shear rate (Figure 3b). From this plot, τ_y is determined at 15 Pa. Such rheological profiles can be attributed to the exist-

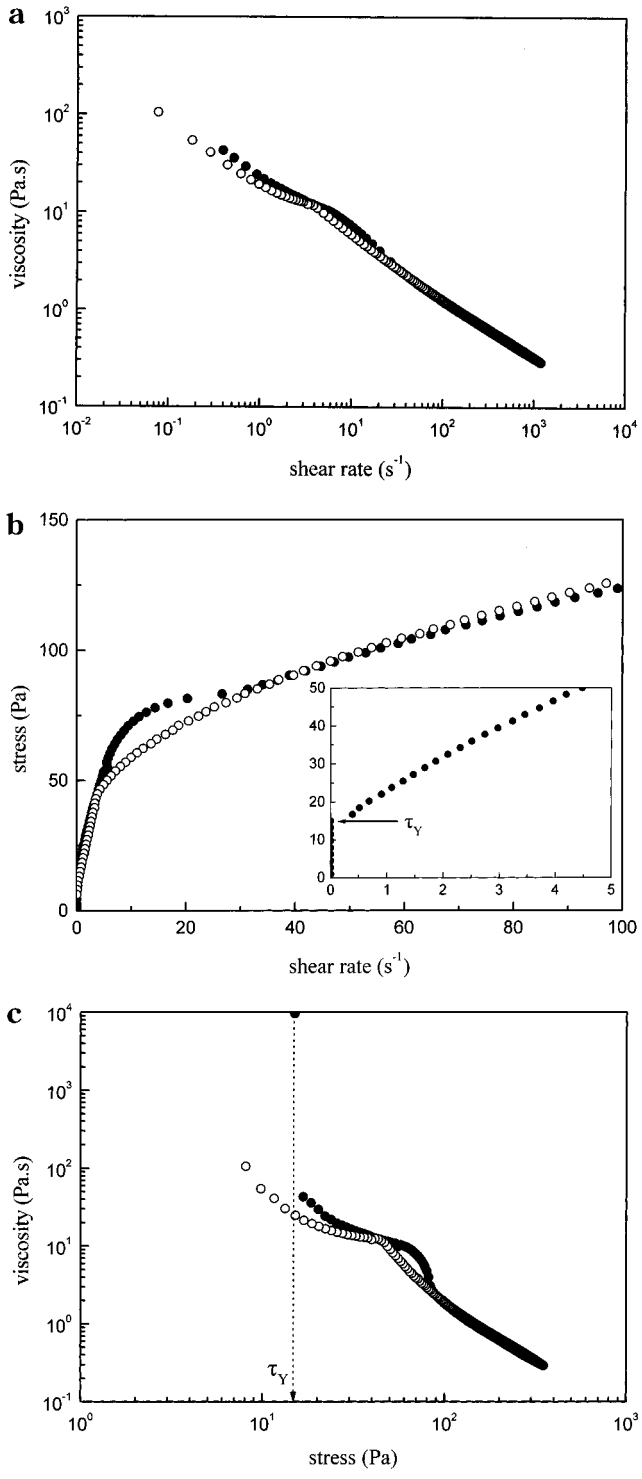

Figure 3. Steady-state shear viscosity data for 1% aqueous solution of PS−PANa−PS: (a) viscosity η versus shear rate $\dot{\gamma}$; (b) shear stress τ versus shear rate $\dot{\gamma}$ (inset: magnification of the low shear rate region); (c) viscosity η versus shear stress τ (the yield stress τ_y is indicated by the dashed arrow). Closed symbols: increasing-τ curve. Open symbols: decreasing-τ curve.

ence of large structures that resist breaking until the applied stress exceeds τ_y. Note also that the curve exhibits a hysteresis loop corresponding to the $\dot{\gamma}$ domain where the discontinuity is observed in Figure 3a.

For such associating systems it has been proposed to plot η as a function of τ—a representation showing more clearly the various transitions and regimes in the flow behavior.[27,32] As shown in Figure 3c, three shear thinning regions can be distinguished. Once the yield stress is exceeded (indicated by the dashed arrow in the figure) the first shear thinning region starts, leading to a smooth decrease in viscosity, up to $\tau \approx 60$ Pa. The second region corresponds to a sharp decrease in viscosity within a narrow shear stress range: $60 < \tau < 80$ Pa. Finally, in a third region, $\tau > 80$ Pa, the viscosity continues to decrease with a higher slope compared to that in the first region. The decreasing shear stress curve is also depicted in Figure 3. Hysteresis phenomena can be observed by comparing the increasing and decreasing stress curves. These phenomena exhibit different magnitudes depending on the shear-thinning region in which they occur. In the third region the up and down curves are practically superimposed. A clear hysteresis is found at $45 < \tau < 80$ Pa, and the sharp transition is not observed anymore; i.e., in the decreasing τ scan the viscosity regularly increases until it meets the up curve at $\tau \approx 45$ Pa. The hysteresis still persists in the first region ($\tau < 45$ Pa). Note also that the decreasing curve continues down to $\tau \approx 7$ Pa, indicating now a lower value for the yield stress. This double-hysteresis effect is reproducible and is observed for $C_P \geq 0.4\%$. All these observations reveal the existence of a transient network structure that is disrupted into large finite associative clusters upon applying a shear stress higher than τ_y. The second discontinuity ($60 < \tau < 80$ Pa) could be attributed to a further breakage or rearrangement of the associative clusters in smaller fragments (see also the discussion in the last section). The recovery of the infinite network structure is not instantaneous. It seems that the global relaxation of the structure occurs in longer time than that of the experiment. Indeed, when the solution is left at rest for ~30 min, it recovers the initial behavior as the new increasing stress curve essentially coincides with the first one.

Plots of the steady-state shear viscosity as a function of shear stress for various polymer concentrations are presented in Figure 4. At concentrations $C_p \leq 0.2\%$ a nearly Newtonian type behavior can be observed. At higher concentrations the viscosity profiles exhibit similar characteristics, namely, a yield stress and a transition region (sharp thinning) at higher τ. The yield stress increases substantially, reminiscent of the behavior of chemically cross-linked gels. This is in agreement with the proposed structure of the present system since the physical cross-links of the network are aggregates of highly hydrophobic, presumably glassy, polystyrene chains. The energy cost to extract a PS end from an aggregate is expected to be much higher than the thermal energy. Obviously at $C_P < 0.4\%$ the network breaks down to separated aggregates or clusters.

Another significant observation arisen from Figure 4 is that the viscosity of the solutions increases several orders of magnitude in a relatively narrow concentration range. In Figure 5, the viscosity (measured at $\dot{\gamma} = 1\ s^{-1}$) is plotted as a function of polymer concentration. Newtonian (zero-shear rate) viscosity cannot be determined due to the existence of yield stress. In the same figure

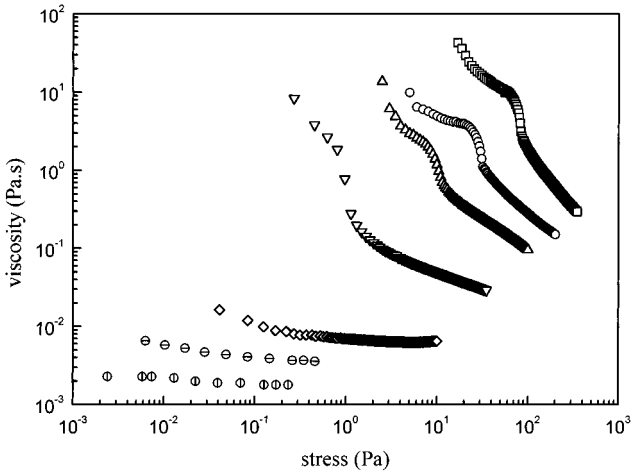

Figure 4. Double-logarithmic plot of steady-state shear viscosity as a function of shear stress for various concentrations of PS−PANa−PS in water: (□) 1.0%, (○) 0.8%, (△) 0.6%, (▽) 0.4%, (◇) 0.2%, (⊖) 0.1%, (Φ) 0.05%.

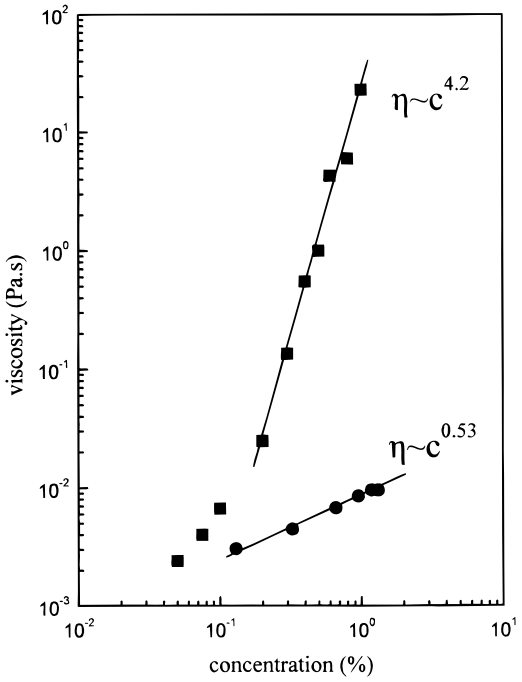

Figure 5. Double-logarithmic plot of the viscosity (measured at $\dot{\gamma} = 1\ s^{-1}$) as a function of concentration for (■) PS−PANa−PS and (○) PANa in aqueous solutions.

the Newtonian viscosity data for poly(sodium acrylate) (PANa) of comparable molecular weight ($M_w = 1.5 \times 10^5$ g/mol) is also presented. The viscosity behavior of the end-capped polymer is characterized by two distinct regions separated to each other by a critical concentration $C_g = 0.2\%$. At $C_P > C_g$ the viscosity increases following the scaling relation $\eta \sim c^{4.2}$. Contrary to that, the viscosity of PANa increases with an exponent of 0.53. The latter is consistent with the theoretical predictions (0.5) concerning the polyelectrolytes in the semidilute unentangled regime.[49] It should mentioned here that the two scaling exponents are not directly comparable since the viscosity data for PS−PANa−PS have been obtained in the shear thinning regime ($\dot{\gamma} = 1\ s^{-1}$).[50] The abrupt increase of η for the end-capped polyelectrolyte is in line with the network model of PS aggregates multiply connected via PANa chains (see

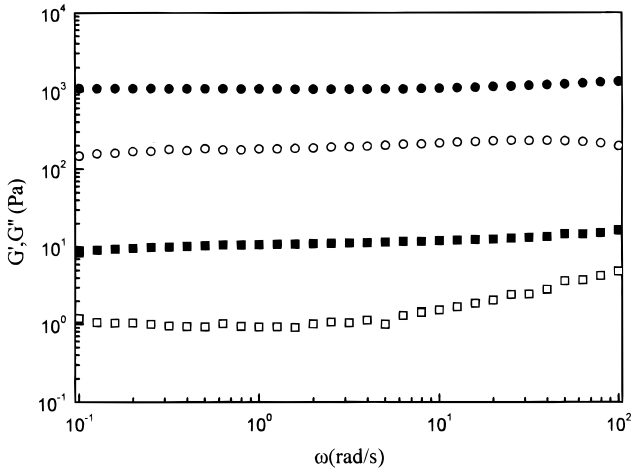

Figure 6. Storage modulus G' (filled symbols) and loss modulus G'' (open symbols) as a function of frequency for PS−PANa−PS aqueous solutions at 1% (circles) and 0.4% (squares) polymer concentration.

discussion in the next section). C_g can be identified as a percolation threshold.[31]

It is interesting to compare the gel concentration C_g with those of other associative end-capped polymers constituted of a nonionic middle block (PEO) and hydrocarbon and/or fluorocarbon end blocks. As has been shown by Mattice et al. by using Monte Carlo simulations, C_g is strongly dependent on the degree of incompatibility, a variable expressing the combined effects of both the size and the solvent insolubility of the end block, but only weakly dependent on the middle block size.[51] Indeed, Francois et al. found $C_g = 1.5\%$ and 4% for $C_{18}-PEO_{455}-C_{18}$ and $C_{12}-PEO_{455}-C_{12}$, respectively.[52] Changing the nature of the hydrophobes from hydrocarbons to fluorocarbons, the latter being more hydrophobic, Xu et al. found $C_g = 2\%$ for $C_8F-PEO_{795}-C_8F$.[6] The PS−PANa−PS of this study exhibits a gel concentration about 1 order of magnitude lower than that of the latter PEO derivative in which the middle block has comparable length. (PEO_{795} has approximately the same contour length as $PANa_{1134}$.) This significant effect could be attributed to two reasons. First the PS_{23} end blocks are much more hydrophobic than the hydrocarbons and/or fluorocarbons, and second the polyelectrolyte middle block is in fully extended form due to the repulsive electrostatic interactions.

Oscillatory Shear Measurements. Oscillatory shear experiments were performed within the linear viscoelastic regime. The storage and the loss moduli as a function of frequency, ω, are plotted for 0.4% and 1% aqueous solutions in Figure 6. Over the entire frequency range studied ($10^{-1}-10^2$ rad/s), G' exceeds G'' by about 1 order of magnitude and is virtually independent of ω, indicating that the solution behaves like a highly elastic gel. Obviously the frequency range examined in the present system is located in the plateau zone of the mechanical spectrum. The terminal zone cannot be explored since the network relaxation time, related to the detachment of a hydrophobe from a junction, is very high (>100 s). That makes a big difference with the end-capped PEO systems for which the relaxation time (at the same C_P) was found ≪100 s.[6,30,53] Note also that in our system the clear elastic character appears for polymer concentrations slightly higher than C_g (i.e., 0.2%). To the best of our knowledge, such elastic behavior has never been observed with hydrophobically end-capped polymers at so low C_P.

Comparison to Previous Studies and Discussion on the Aggregation Mechanism. As shown in the fluorescence section, the copolymer PS−PANa−PS forms hydrophobic micellar type aggregates at polymer concentrations lower than 0.1%. Most probably the cac is of the order of 0.002% as can be concluded by comparing to the data on diblock PS−PANa copolymers.[43]

The question to answer now relates to the nature of the micelles in the relatively dilute regime, i.e., cac < C_P < C_g = 0.2%. For associative PEO with highly hydrophobic ends the formation of flower-type micelles has been suggested. In that case the PEO chains form loops that constitute the hydrophilic corona of the micelle. The stability of the flower micelles has been discussed in details by Xu et al.[6] They used the thermodynamic criterion proposed by Raspaud et al.[54,55] Within this model the loop is formed only when the entropy penalty due to the middle block backfolding is balanced by the energy gain due to the transferring of the hydrophobic chain end from the aqueous solvent into the micellar core. In the triblock copolymer used in this work the middle block is a long and highly charged polyelectrolyte that makes the backfolding of the chain rather unfavorable. A comparison can be done with diblock copolymers based on a short hydrophobic block and a long polyelectrolyte chain. These copolymers form micelles in the hydrophilic coronas of which the polyelectrolyte blocks are essentially fully extended.[56−58] Such extended conformation has also been predicted theoretically for micelles[59] and star-branched polyelectrolytes.[60] From the above arguments we can conclude that in the concentration regime between cac and C_g our triblock copolymer forms a kind of loose multimicellar clusters constituted of starlike micelles connected via extended PANa chains (Figure 7a). We must note here that the presence of loops is not excluded, but at the present stage of understanding of the system we cannot conclude on the relative fraction of loops and bridges.

Because of the expected extensive bridging between the starlike micelles, one would have also expect the formation of a macroscopic network in equilibrium with excess solvent at C_P < C_g. However, such a phase separation is not observed in this system when pure water is used as solvent. Obviously electrostatic repulsive interactions between the multimicellar clusters operate against the macroscopic phase separation. When salt is added to the system, the electrostatic interactions are screened and phase separation appears. For instance, the relative volume of the gellike polymer-rich phase as a function of NaCl concentration is shown in Figure 8 (C_P = 0.5%). Note that the phase behavior of associating end-capped polyelectrolytes has been described theoretically in a recent work.[61] The model predictions on the salt effect are in agreement with our observation.

Let us now come back to the discussion of the behavior in pure water. When increasing C_P, percolation of the clusters starts and the gel behavior appears. It is likely that some bridging between clusters occurs via stretched polymer chains. As a consequence, in the concentration range just above C_g the system is expected to be heterogeneous in a mesoscopic level: between the clusters there are regions of low polymer concentration. The higher the C_P, the more homogeneous becomes the

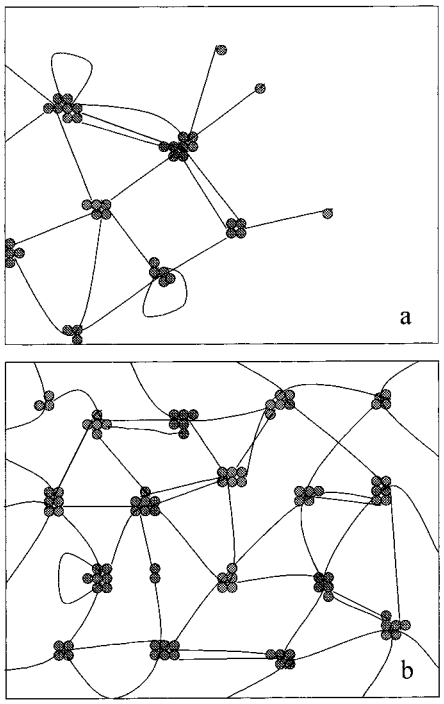

Figure 7. Representation of possible association structures of PS−PANa−PS in aqueous solutions: (a) loose multimicellar clusters at cac < C_P < C_g; (b) transient network at C_P > C_g. PS aggregates and PANa chains are not drawn to scale. The number of PS ends per aggregate is expected to be high (see ref 48).

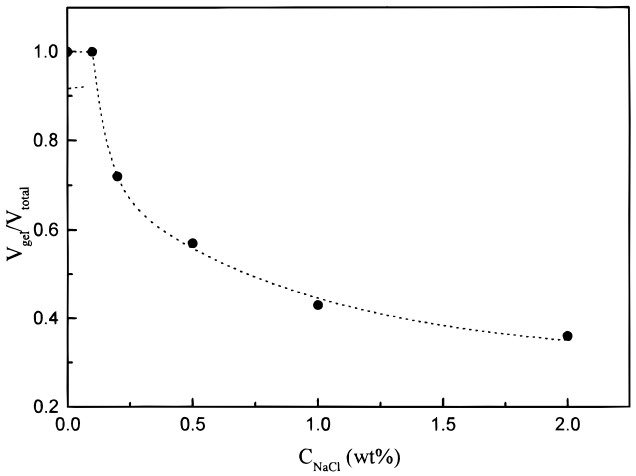

Figure 8. Effect of salt (NaCl) on the relative volume, V_{gel}/V_{total} of the polymer-rich phase for a 0.5% aqueous solution of PS−PANa−PS; T = 20 °C.

network (Figure 7b). This association model is in line with the experimental observations of this work, namely the low C_g, the high G_0, and the discontinuity in the flow properties (Figures 3−6). Compared to hydrophobically end-capped PEO,[6,30,52,53] our copolymer exhibits a C_g about 1 order of magnitude lower, attributed to the stretched long PANa blocks and to the high hydrophobicity of the PS ends.

For other end-capped associating polymers the plateau modulus, G_0, has been related to the number density of elastically active chains ν through the relation

$$G_0 = \nu k_B T \qquad (1)$$

For end-capped PEO, ν was found to be clearly lower than the total number density n of chains in the solution, i.e., $\nu/n \ll 1$.[23,30,53] Although eq 1 cannot be directly applied to our system because of the expected stretched conformation and the polyelectrolyte nature of PANa middle block, we will use it here in order to get just a qualitative comparison to previously reported PEO systems. From the data of Figure 6 we find ν/n = 0.1 and 3.5 for C_P = 0.4% and 1%, respectively. These high ν/n values can be taken as an extra indication of favored bridging, toward looping, in the present system. Another characteristic of the present system is the very long relaxation time (clearly longer than 100 s) as revealed from the data of Figure 6.

Before ending we would like to briefly discuss the flow behavior of this system (Figures 3 and 4). As stated above, the system is expected to be heterogeneous on a mesoscopic level. Upon applying increasing stress, some bridges between clusters are broken first and the system starts to flow (yield stress). At higher stresses, or shear rates, some rearrangement occurs even inside the clusters, and that might explain the transition (discontinuity) observed at $\tau > \tau_y$. An interesting observation is that the flow behavior is, at least partially, reversible. The return curve (decreasing τ) exhibits an hysteresis around the discontinuity point, and the apparent yield stress is now lower. The system approximately recovers its initial behavior if allowed at rest for ∼30 min. The new increasing τ curve is essentially identical to the first one. This slow reversibility is in line with the estimation of a very long relaxation time, and moreover it indicates that the system is not fully frozen despite the relatively high $T_g \approx 55$ °C of the PS_{23} ends.[37] A similar conclusion on not frozen structure for micelles of PS_{23}−$PANa_{300}$ diblock copolymers has been reported by Khougaz et al.[58]

To confirm the above mechanism, further work is now in progress: dynamic viscoelasticity and light scattering studies.

Conclusions

Well-defined model A−B−A triblock copolymers constituted from a polyelectrolyte middle block and PS end blocks were synthesized by anionic polymerization and characterized adequately by various techniques. The synthetic route followed provides that all polyectrolyte chains bear at both ends short PS hydrophobes.

In dilute aqueous solutions and at low concentrations these amphiphiles form "star"-like micelles interconnected via the extended polyelectrolyte blocks to give loose multimicellar clusters. At relatively higher polymer concentrations, but still lower than 1%, a second level of association occurs, leading to the formation of a network as revealed by the viscoelastic behavior of the system. This is attributed to extensive bridging of the star micelles via the stretched PANa blocks (see Figure 7b).

The concentration at which the gel properties appear, C_g = 0.2%, is remarkably lower than that found for other end-capped polymers. The steady shear viscosity profile at $C_P > C_g$ reveals a rather complex rheological behavior (yield stress, sharp thinning at higher stresses). Moreover, the system seems to have a very long relaxation time, >100 s, and only the plateau zone can be observed in the oscillatory shear experiments.

Details of the viscoelastic behavior of the system will appear in a forthcoming paper. Further work is in

progress in an attempt to explore the influence of the nature and the length of the end blocks.

Acknowledgment. C.T. expresses his gratitude to the University P. et M. Curie for invited professorship during June 1999. We thank Sergei Obukhov, Françoise Lafuma, and Dominique Hourdet for stimulating discussions and Dimitris Voulgaris for his assistance in the synthesis of the triblock copolymers.

References and Notes

(1) Laschewsky, A. *Adv. Polym. Sci.* **1995**, *124*, 1.
(2) Winnik, M. A.; Yekta, A. *Curr. Opin. Colloid Interface Sci.* **1997**, *2*, 424.
(3) Glass, J. E. *Water-Soluble Polymers: Beauty with Performance*; American Chemical Society: Washington, DC, 1986; Vol. 213.
(4) Xie, X.; Hogen-Esch, T. E. *Macromolecules* **1996**, *29*, 1734.
(5) Petit, F.; Iliopoulos, I.; Audebert, R.; Szönyi, S. *Langmuir* **1997**, *13*, 4229.
(6) Xu, B.; Li, L.; Yekta, A.; Masoumi, Z.; Kanagalingam, S.; Winnik, M. A.; Zhang, K.; Macdonald, P. M.; Menchen, S. *Langmuir* **1997**, *13*, 2447.
(7) Biggs, S.; Hill, A.; Selb, J.; Candau, F. *J. Phys. Chem.* **1992**, *96*, 1505.
(8) Hill, A.; Candau, F.; Selb, J. *Macromolecules* **1993**, *26*, 4521.
(9) Volpert, E.; Selb, J.; Candau, F. *Macromolecules* **1996**, *29*, 1452.
(10) McCormick, C. L.; Nonaka, T.; Johnson, C. B. *Polymer* **1988**, *29*, 731.
(11) Ezzell, S. A.; McCormick, C. L. *Macromolecules* **1992**, *25*, 1881.
(12) Ringsdorf, H.; Venzmer, J.; Winnik, F. M. *Macromolecules* **1991**, *24*, 1678.
(13) Seery, T. A. P.; Yassini, M.; Hogen-Esch, T. E.; Amis, E. J. *Macromolecules* **1992**, *25*, 4784.
(14) Uemura, Y.; McNulty, J.; Macdonald, P. M. *Macromolecules* **1995**, *28*, 4150.
(15) Xu, B.; Li, L.; Zhang, K.; Macdonald, P. M.; Winnik, M. A.; Jenkins, R.; Bassett, D.; Wolf, D.; Nuyken, O. *Langmuir* **1997**, *13*, 6896.
(16) Wang, T. K.; Iliopoulos, I.; Audebert, R. *Polym. Bull.* **1988**, *20*, 577.
(17) Wang, T. K.; Iliopoulos, I.; Audebert, R. In *Water-Soluble Polymers. Synthesis Solution Properties and Applications*; Shalaby, S. W., McCormick, C. L., Butler, G. B., Eds.; ACS Symposium Series 467; American Chemical Society: Washington, DC, 1991; p 218.
(18) Tam, K. C.; Farmer, M. L.; Jenkins, R. D.; Bassett, D. R. *J. Polym. Sci., Part B: Polym. Phys.* **1998**, *36*, 2275.
(19) Tirtaatmadja, V.; Tam, K. C.; Jenkins, R. D. *Macromolecules* **1997**, *30*, 1426.
(20) Branham, K. D.; Davis, D. L.; Middleton, J. C.; McCormick, C. L. *Polymer* **1994**, *35*, 4429.
(21) Hu, Y.; Smith, G. L.; Richardson, M. F.; McCormick, C. L. *Macromolecules* **1997**, *30*, 3526.
(22) Kevelam, J.; Engberts, J. B. F. N. *J. Colloid Interface Sci.* **1996**, *178*, 87.
(23) Xu, B.; Yekta, A.; Li, L.; Masoumi, Z.; Winnik, M. A. *Colloids Surf., A* **1996**, *112*, 239.
(24) Alami, E.; Rawiso, M.; Isel, F.; Beinert, G.; Binana-Limbele, W.; Francois, J. In *Hydrophilic Polymers: Performance with Environmental Acceptance*; Glass, J. E., Ed.; Advances in Chemistry Series 248; American Chemical Society: Washington, DC, 1996; p 343.
(25) Jenkins, R. D.; Silebi, C. A.; El-Aasser, M. S. *Polym. Mater. Sci. Eng.* **1989**, *61*, 629.
(26) Chassenieux, C.; Nicolai, T.; Durand, D. *Macromolecules* **1997**, *30*, 4952.
(27) Tam, K. C.; Jenkins, R. D.; Winnik, M. A.; Bassett, D. R. *Macromolecules* **1998**, *31*, 4149.
(28) Abrahmsen-Alami, S.; Persson, K.; Stilbs, P.; Alami, E. *J. Phys. Chem.* **1996**, *100*, 4598.
(29) Alami, E.; Almgren, M.; Brown, W.; Francois, J. *Macromolecules* **1996**, *29*, 2229.
(30) Annable, T.; Buscall, R.; Ettelaie, R. *Colloids Surf., A* **1996**, *112*, 97.
(31) Semenov, A. N.; Joanny, J. F.; Khokhlov, A. R. *Macromolecules* **1995**, *28*, 1066.
(32) English, R. J.; Gulati, H. S.; Jenkins, R. D.; Kahn, S. A. *J. Rheol.* **1997**, *41*, 427.
(33) Petit, F.; Iliopoulos, I. *J. Phys. Chem. B* **1999**, *103*, 4803.
(34) Petit, F.; Iliopoulos, I.; Audebert, R. *Polym. Commun.* **1998**, *39*, 751.
(35) Valint, P. L. J.; Bock, J. *Macromolecules* **1988**, *21*, 175.
(36) Murphy, A.; Hill, A.; Vincent, B. *Ber. Bunsen-Ges. Phys. Chem.* **1996**, *100*, 963.
(37) O'Driscoll, K.; Amin Sanayei, R. *Macromolecules* **1991**, *24*, 4479.
(38) Moffitt, M.; Khougaz, K.; Eisenberg, A. *Acc. Chem. Res.* **1996**, *29*, 95.
(39) Hautekeer, J. P.; Varshney, S. K.; Fayt, R.; Jacobs, C.; Jérôme, R.; Teyssié, P. *Macromolecules* **1990**, *23*, 3893.
(40) Fayt, R.; Forte, R.; Jacobs, C.; Jérôme, R.; Ouhadi, T.; Teyssié, P.; Varshney, S. K. *Macromolecules* **1987**, *20*, 1442.
(41) Gnanou, Y. *Polymer* **1994**, *35*, 4011.
(42) Rager, T.; Meyer, W. H.; Wegner, G.; Winnik, M. A. *Macromolecules* **1997**, *30*, 4911.
(43) Astafieva, I.; Zhong, X. F.; Eisenberg, A. *Macromolecules* **1993**, *26*, 7339.
(44) Wilhelm, M.; Zhao, C. L.; Wang, Y.; Xu, R.; Winnik, M. A.; Mura, J. L.; Riess, G.; Croucher, M. D. *Macromolecules* **1991**, *24*, 1033.
(45) Kalyanasundaram, K.; Thomas, J. K. *J. Am. Chem. Soc.* **1977**, *99*, 2039.
(46) Zana, R. In *Surfactant Solutions: New Methods of Investigation*; Zana, R., Ed.; Surfactant Science Series 22; Marcel Dekker: New York, 1987; p 241.
(47) Anthony, O.; Zana, R. *Macromolecules* **1994**, *27*, 3885.
(48) Astafieva, I.; Khougaz, K.; Eisenberg, A. *Macromolecules* **1995**, *28*, 7127.
(49) Dobrynin, A. V.; Colby, R. H.; Rubinstein, M. *Macromolecules* **1995**, *28*, 1859.
(50) Boris, D. C.; Colby, R. H. *Macromolecules* **1998**, *31*, 5746.
(51) Nguyen-Mirsa, M.; Mattice, W. L. *Macromolecules* **1995**, *28*, 1444.
(52) Francois, J.; Maitre, S.; Rawiso, M.; Sarazin, D.; Beinert, G.; Isel, F. *Colloids Surf. A: Physicochem. Eng. Asp.* **1996**, *112*, 251.
(53) Cathébras, N.; Collet, A.; Viguier, M.; Berret, J. F. *Macromolecules* **1998**, *31*, 1305.
(54) Raspaud, E.; Lairez, D.; Adam, M.; Carton, J. P. *Macromolecules* **1994**, *27*, 2956.
(55) Raspaud, E.; Lairez, D.; Adam, M.; Carton, J. P. *Macromolecules* **1996**, *29*, 1269.
(56) Guenoun, P.; Davis, H. T.; Tirrell, M.; Mays, J. W. *Macromolecules* **1996**, *29*, 3965.
(57) Guenoun, P.; Delsanti, M.; Gazeau, D.; Mays, J. W.; Cook, D. C.; Tirrell, M.; Auvray, L. *Eur. Phys. J. B* **1998**, *1*, 77.
(58) Khougaz, K.; Astafieva, I.; Eisenberg, A. *Macromolecules* **1995**, *28*, 7135.
(59) Shusharina, N. P.; Nyrkova, I. A.; Khokhlov, A. R. *Macromolecules* **1996**, *29*, 3167.
(60) Borisov, O. V.; Zhulina, E. B. *Eur. Phys. J. B* **1998**, *4*, 205.
(61) Vasilevskaya, V. V.; Potemkin, I. I.; Khokhlov, A. R. *Langmuir* **1999**, *15*, 7918.

MA991410E